Title

Inhibition of Hexavalent Chromium Release from Drinking Water Distribution Systems: Effects of Water Chemistry-Based Corrosion Control Strategies.

Journal

Environmental Science & Technology, 57(47)

Authors

Tan, Cheng

Liu, Haizhou

Publication Date

2023-11-28

DOI

10.1021/acs.est.2c05324

Peer reviewed

Environmental Science & Technology

pubs.acs.org/est

Article

Inhibition of Hexavalent Chromium Release from Drinking Water Distribution Systems: Effects of Water Chemistry-Based Corrosion Control Strategies

Cheng Tan and Haizhou Liu*

Cite This: *Environ. Sci. Technol.* 2023, 57, 18433−18442

Read Online

ACCESS | Metrics & More | Article Recommendations | Supporting Information

ABSTRACT: In drinking water distribution systems, the oxidation of zerovalent chromium, Cr(0), in iron corrosion scales by chlorine residual disinfectant is the dominant reaction to form carcinogenic hexavalent chromium, Cr(VI). This study investigates inhibitive corrosion control strategies through adjustments of chemical water parameters (i.e., pH, silicate, phosphate, calcium, and alkalinity) on Cr(VI) formation through oxidation of $Cr(0)_{(s)}$ by free chlorine under drinking water conditions. The results show that an increase in pH, silicate, alkalinity, and calcium suppressed Cr(VI) formation that was mainly attributed to in situ surface precipitation of new Cr(III) solids on the surface of $Cr(0)_{(s)}$, including $Cr(OH)_{3(s)}$, $Cr_2(SiO_3)_{3(s)}$, $CrPO_{4(s)}$, $Cr_2(CO_3)_{3(s)}$, and $Cr_{10}Ca(CO_3)_{16(s)}$. The Cr(III) surface precipitates were much less reactive with chlorine than $Cr(0)_{(s)}$ and suppressed the Cr redox reactivity. The concentration of surface Cr(III) solids was inversely correlated with the rate constant of Cr(VI) formation. Adding phosphate either promoted or inhibited the Cr(VI) formation, depending on the phosphate concentration. This study provides fundamental insight into the Cr(VI) formation mechanisms via Cr(0) oxidation by chlorine and the importance of surface precipitation of Cr(III) solids with different corrosion control strategies and suggests that increasing the pH/alkalinity and addition of phosphate or silicate can be effective control strategies to minimize Cr(VI) formation.

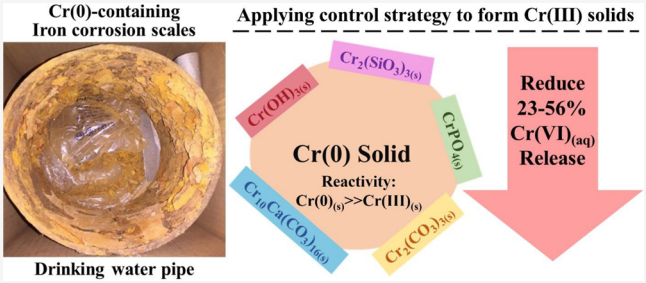

KEYWORDS: *chromium, carcinogen, free chlorine, corrosion, redox reactivity, drinking water*

INTRODUCTION

Chromium exists in one of three stable oxidation states in the environment, including zerovalent chromium, Cr(0), trivalent chromium, Cr(III), and hexavalent chromium, Cr(VI).[1] In drinking water with a pH above 6.5, Cr(VI) in the form of carcinogenic CrO_4^{2-} is the dominant dissolved Cr species (chromic acid: pK_{a1} = 0.7 and pK_{a2} = 6.5).[2−4] The current maximum contaminant level (MCL) for total Cr established by the U.S. EPA is 100 μg/L.[5] A Public Health Goal (PHG) for Cr(VI) was set at 0.02 μg/L by the Office of Environmental Health Hazard Assessment in California.[6] The Cr(VI) concentration in U.S. drinking water was measured to be between 0.057 and 7.51 μg/L based on results from the 2018−2020 U.S. EPA Round 4 Unregulated Contaminant Monitoring Rule Program (UCMR4).[7]

The sources of Cr(VI) in drinking water include anthropogenic industrial waste discharges and natural geological weathering of Cr-containing minerals.[8−11] Cr(VI) can be effectively removed from drinking water by reductive coagulation and filtration, ion exchange, adsorption, or membrane filtration.[12,13] However, Cr(0) in its metallic form is commonly used in iron-based corrosion-resistant alloys such as cast iron and steel materials.[8] Cast iron pipes (1−4% Cr(0)) and steel pipes (≥11% Cr(0)) together account for approximately 60% of all piping materials in drinking water distribution systems (DWDSs) in the United States.[14] Reactions between disinfectants and aging iron pipes can lead to the release of Cr(VI) in drinking water.[15] Analysis of the UCMR4 database also showed that more than 40% of the drinking water that left distribution systems had increased in Cr(VI) concentration relative to the entry point.[16]

Cr(0) solid was recently discovered to exist in iron corrosion scales and significantly contributed to Cr(VI) formation by oxidative conversion to Cr(VI) by the residual free chlorine (denoted HOCl as the dominant species at pH 7 in the following text) in DWDSs.[15] The Cr(0) in the cast iron pipe material exhibited approximately 2 orders of magnitude higher

Special Issue: Oxidative Water Treatment: The Track Ahead

Received: July 25, 2022
Revised: January 11, 2023
Accepted: January 12, 2023
Published: January 31, 2023

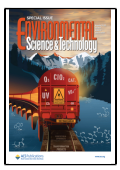

reactivity with HOCl than Cr(III) hydroxide-based solids in the iron corrosion scales.[15]

Little knowledge exists on how to inhibit the Cr(0) redox reactivity to minimize Cr(VI) formation. Traditionally, adjustment of chemical parameters has been employed or proposed as an effective corrosion strategy to minimize metal release from DWDSs. For example, pH and alkalinity adjustment have been used for iron corrosion control, which can be accomplished by aeration and chemical dosing, including lime $Ca(OH)_2$ and soda ash Na_2CO_3.[17,18] Raising the pH to 8 was reported to effectively control iron, lead, and copper corrosion,[19−21] as a higher pH can favor the formation of a passivation layer.[22] Water pH can significantly impact the speciation of surface hydroxo complexes of Cr(III) solids and the speciation of chlorine that in turn can affect the reaction kinetics of Cr(VI) formation through the oxidation of Cr(III) solids by HOCl.[23,24] Alkalinity also can significantly influence the corrosion of metallic pipes and release different metals including iron and lead in DWDSs.[19,25,26] High calcium and alkalinity can lead to calcium carbonate precipitation that acts as a passivation layer to inhibit lead and copper corrosion.[27,28] However, the effectiveness of alkalinity and calcium on the control of chromium release is unknown.

Furthermore, phosphate and silicate can be used as corrosion inhibitors and sequestrants.[29,30] Adding phosphate effectively controls lead corrosion by forming Pb phosphate solids that have an extremely low solubility.[31] Silicate has been shown to reduce lead and copper levels and may form an adherent film on the surface of the pipe that acts as a diffusion barrier.[32] Silicate has also been used as corrosion inhibitor in iron-based water pipes, as silicate can complex Fe^{2+} and form a passivation layer of $FeSiO_{3(s)}$.[33]

However, drinking distribution systems are highly complex; thus, a particular control strategy may be system specific. For example, it was reported that both weight loss and iron concentration decreased on increasing the pH from 8.5 to 9.2, and red water was received when the alkalinity was maintained at higher values.[34] Higher levels of silica can cause more iron release to the water and decreased the size of suspended iron particles.[35]

Currently, very little is known on how significant the adjustment of these water chemistry parameters as corrosion control strategies can affect the surface redox reaction between Cr(0) solid and HOCl. Filling this knowledge gap is critical to understand and control Cr(VI) formation in water from DWDSs. Accordingly, the objectives of this study were (1) to investigate the reaction kinetics and mechanisms of $Cr(0)_{(s)}$ oxidation by chlorine in conjunction with different corrosion control strategies based on adjustments of chemical water parameters (i.e., pH, silicate, phosphate, calcium, and alkalinity) and (2) to explore new control strategies to inhibit Cr(VI) release from DWDSs. A thorough understanding of the influence of these water parameters on Cr(VI) formation is essential to develop Cr(VI) control strategies in different drinking water distribution infrastructures.

MATERIALS AND METHODS

Chemicals. All chemicals used in this study were reagent grade or higher. All solutions were freshly prepared using deionized water (>18.2 MΩ·cm, Millipore System). $Cr(0)_{(s)}$ with a uniform particle size of 10 μm was purchased from Sigma-Aldrich. The chlorine working solution (HOCl) was prepared freshly using a NaOCl stock solution. Four Cr(III) reference solids, including $CrPO_{4(s)}$, $Cr_2(SiO_3)_{3(s)}$, $Cr_2(CO_3)_{3(s)}$, and $Cr_{10}Ca(CO_3)_{16(s)}$, were synthesized by a precipitation method. The detailed synthesis procedure and characterization information is given in Text S1 of the Supporting Information (SI).

Oxidation Experiments of Cr(0) Solid by Chlorine. A 200 mL suspension containing 440 mg/L (8.5 mM) $Cr(0)_{(s)}$ was mixed with 20 mg of Cl_2/L (0.28 mM) of HOCl in a 250 mL glass vessel in the dark. HOCl at 20 mg Cl_2/L was used instead of the lower concentration in DWDSs (<2 mg/L Cl_2/L) because the higher concentration provides valuable insight into the oxidation kinetics, while the kinetics and mechanisms obtained at high-concentration conditions can be extrapolated to predict reactions at low-concentration conditions.[15,36,37] The oxidation experiment was conducted for 6 h. The chemical parameters were varied to reflect different drinking water conditions, including pH (6−8), silicate (0−10 mg/L), phosphate (0−10 mg/L), calcium (0−300 mg/L), and alkalinity (0−200 mg $CaCO_3$/L). The pH of the suspension was maintained throughout the reaction with a Eutech Instrument Alpha pH200 controller. The concentrations of silicate, phosphate, calcium, and alkalinity were prepared by adding Na_2SiO_3, Na_3PO_4, $CaCl_2$, and $NaHCO_3$ stock solutions, respectively. After HOCl is dosed into the reactor, 5 mL of the suspension was collected every 30 min and filtrated through a 0.22 μm filter (nylon membrane, Agilent). The HOCl in the filtrate was immediately quenched with excess $(NH_4)_2SO_4$, and the total amounts of Cr and Cr(VI) were measured. This followed an established protocol for sample pretreatment.[15] An additional 0.5 mL of suspension was collected every 2 h, filtered through 0.22 μm filters, diluted by 10 times, and quantified for HOCl concentration. In addition to kinetic studies with Cr(0), the oxidation of four Cr(III) reference solids by HOCl was conducted at pH 7 as a control.

Acid Digestion and Solubility Experiments of Cr(III) Solid. To quantify the amount of in situ surface precipitation of Cr(III) solids during $Cr(0)_{(s)}$ oxidation by HOCl, solids were collected and acid digested by EPA Method 3050B after the 6 oxidation reaction.[38] The brief principal was that HNO_3 and 30% H_2O_2 can dissolve Cr(III) solids with heating at 95 °C. In brief, after a 6 h reaction, the suspension was quenched with excess $(NH_4)_2SO_4$ and centrifuged for 10 min. The Cr solids were washed twice with DI water and centrifuged to efficiently remove the adsorbed ions. The final Cr solids were freeze dried and digested. In addition, the $Cr(0)_{(s)}$ from a control experiment without free chlorine was digested to deduct the background of any residual of adsorbed ions. This was proved to be a reliable method to quantify Cr(III) solids without inference from $Cr(0)_{(s)}$ because EPA Method 3050B can completely dissolve Cr(III) solids and cannot dissolve Cr(0) solid.[15] The concentrations of Cr, P, and Si in the digested solution were analyzed using ICP-MS to quantify the Cr(III) solid species on the surface of $Cr(0)_{(s)}$.

In addition, control experiments to evaluate the adsorption of Cr(VI) onto $Cr(0)_{(s)}$ were conducted by dosing 0.1−1 mg/L Cr(VI) using potassium dichromate ($K_2Cr_2O_7$) in a 0.44 g/L Cr(0) suspension. After 6 h, the aqueous Cr(VI) concentration was quantified by Method 3050B. On the basis of the mass balance, the percentage of Cr(VI) adsorbed on $Cr(0)_{(s)}$ was calculated. The adsorption of Cr(VI) on $Cr(0)_{(s)}$ was negligible after 6 h adsorption at pH 6−8 (Figure S1); therefore, Cr(VI) adsorption did not interfere with the

https://doi.org/10.1021/acs.est.2c05324
Environ. Sci. Technol. 2023, 57, 18433−18442

quantification of precipitated Cr(III) solids on the surface of $Cr(0)_{(s)}$.

To further understand the Cr(III) solid formation under different water chemistry, the solubility product constant (K_{sp}) for each synthesized Cr(III) reference solid was quantified based on a 6 h dissolution experiment. The dissolution time was chosen as 6 h because the dissolved Cr(III) concentrations reached plateaus at 6 h as shown in Figure S2. Briefly, the suspension with 0.1 g/L of each Cr(III) reference solid was stirred at 700 rpm for 6 h, and then, the dissolved Cr that can pass through a 0.22 μm filter (nylon membrane, Agilent) was quantified and used to calculate the K_{sp} (detailed information in Text S2). All experiments were conducted at 25 °C.

Analytical Methods. Cr(VI) concentration was measured using the standard diphenylcarbazide (DPC) method with a spectrophotometer.[39] The brief principal was that DPC reacted with Cr(VI) to form the colored Cr(VI)−DPC complex, and the absorbance of the solution was then measured at 540 nm. HOCl concentrations were measured using the standard DPD method.[39] The concentrations of dissolved Cr, Si, P, and Ca were analyzed using inductively coupled plasma mass spectrometry (ICP-MS, Agilent 7700). Ca was measured under the hydrogen mode to reduce interference.[40] The Brunauer−Emmett−Teller (BET) surface areas of Cr(0) and Cr(III) solids were measured using a Micromeritics ASAP 2020 surface area analyzer. All experiments were conducted in duplicate, and the error bars were calculated accordingly. Two-way ANOVA statistical analysis was conducted using Software R (v4.0.3) to test the significant difference for the effects of pH and silicate on Cr(VI) formation.

Modeling of Reaction Kinetics. The reaction rate constant of Cr(VI) formation ($k_{Cr(VI)}$) via $Cr(0)_{(s)}$ oxidation by chlorine was obtained by fitting experimental data of Cr(VI) release using the software OpenModel. A second-order reaction kinetics model was introduced to quantify the reaction rate constant of Cr(VI) formation ($k_{Cr(VI)}$) based on eq 1

$$\frac{d[Cr(VI)]}{dt} = k_{Cr(VI)}[Cr_{(s)}][HOCl](S_{Cr(0)})(AW_{Cr}) \quad (1)$$

where $k_{Cr(VI)}$ is the surface-area normalized second-order rate constant for Cr(VI) formation from Cr(0) powder ($L \cdot m^{-2} \cdot min^{-1}$), [HOCl] is the HOCl concentration (mol/L) at any reaction time t (min), $[Cr_{(s)}]$ is the Cr solids concentration (mol/L), $S_{Cr(0)}$ is the $Cr(0)_{(s)}$ BET surface area (m^2/g), and AW_{Cr} is Cr atomic weight of 52 g/mol. $[Cr_{(s)}]$ is the initial $Cr(0)_{(s)}$ concentration minus the dissolved Cr(VI) concentration at time t.

All of the data for the Cr(VI) concentrations and free chlorine concentrations at different time points were input into the model. $k_{Cr(VI)}$ was an experimentally observed rate constant combining both the one-step oxidation of $Cr(0)_{(s)}$ to Cr(VI) and the oxidation of $Cr(III)_{(s)}$ to Cr(VI). All modeled fitting curves matched the observed Cr(VI) concentrations well with R^2 ranging between 0.972 and 0.996.

To evaluate the control strategies for Cr(VI) release in DWDSs dominated by iron pipe, a kinetics model was established using the reaction rate constants ($k_{Cr(VI)}$) obtained from this study (with details of the model found in Text S3). The relative Cr(VI) formation was predicted based on typical drinking water conditions, and it was calculated by dividing the Cr(VI) formation under one certain water condition by Cr(VI) formation at pH 6 with only Cr solid and free chlorine.

RESULTS AND DISCUSSION

Effect of pH on Cr(VI) Formation. The redox potential of $Cr(VI)/Cr(0)_{(s)}$ (−1.49 V) is lower than that of $HOCl/Cl^-$ (1.25 V) in typical drinking water chemical conditions;[15] thus, the overall oxidation of $Cr(0)_{(s)}$ to Cr(VI) by HOCl is thermodynamically feasible as

$$Cr(0)_{(s)} + 3HOCl + H_2O \rightarrow CrO_4^{2-} + 5H^+ + 3Cl^- \quad (R1)$$

Cr(VI) formation decreased with increasing pH from 6 to 8 (Figure 1A). Statistical analysis showed that compared to the

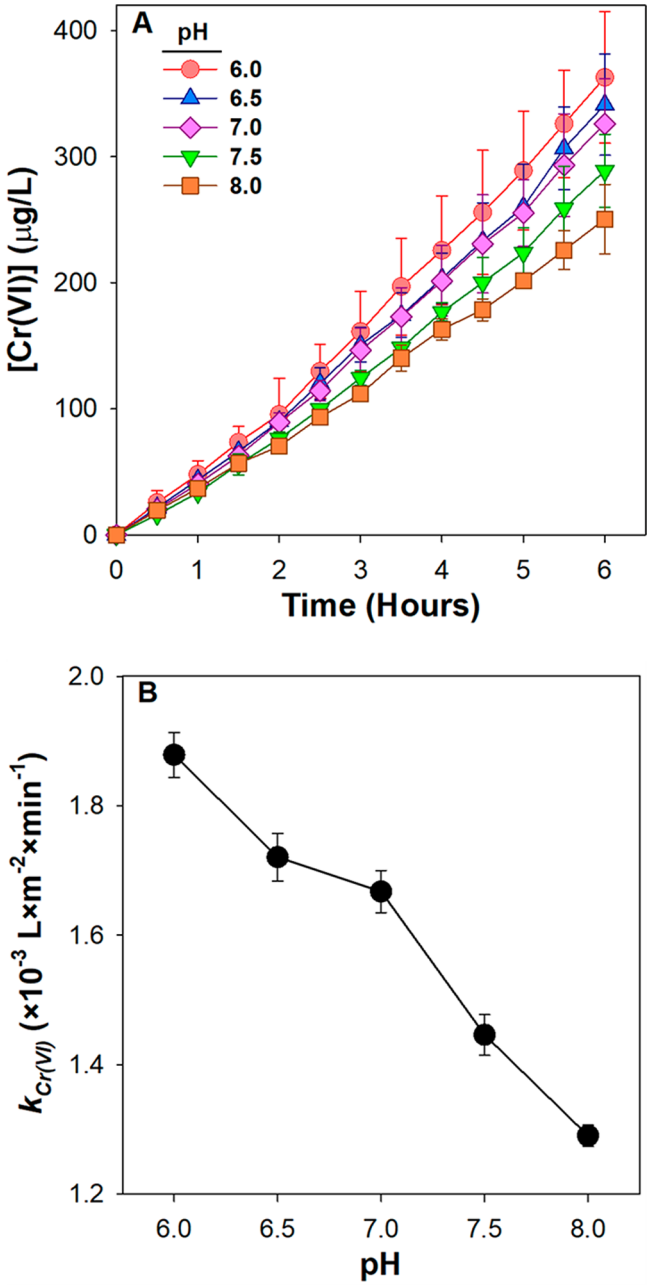

Figure 1. Six hour oxidation of $Cr(0)_{(s)}$ by free chlorine at different pH levels. $[HOCl]_{TOT}$ = 20 mg Cl_2/L (0.282 mM); $[Cr(0)_{(s)}]$ = 440 mg/L (8.46 mM); molar ratio of Cr(0)/HOCl = 30:1; ionic strength = 10 mM, [Ca] = 0 mg/L. (A) Cr(VI) formation; (B) $k_{Cr(VI)}$. p value for Cr(VI) formation compared to that at pH 7: pH 6 (0.0105), pH 6.5 (0.9890), pH 7.5 (0.0066), and pH 8 (<0.0001).

https://doi.org/10.1021/acs.est.2c05324
Environ. Sci. Technol. 2023, 57, 18433−18442

Cr(VI) formation at pH 7, all pH values had significant effects on Cr(VI) formation except for pH 6.5. Correspondingly, surface-area-normalized rate constants of Cr(VI) formation ($k_{Cr(VI)}$) decreased by 31% from 1.9×10^{-3} to 1.3×10^{-3} L·m^{-2}·min^{-1} (Figure 1B). During the oxidation reaction, the Cr(III) solid concentration on the surface of $Cr(0)_{(s)}$ increased from 0.17 to 0.47 mg/g when the solution pH increased from 6 to 8 (Figure S3); thus, a higher pH resulted in an enhanced Cr(III) solid formation on the surface of $Cr(0)_{(s)}$. CO_2 in air has a negligible effect on the $Cr(III)_{(s)}$ formation. At pH 7, the carbonate in equilibrium with headspace air in the reactor resulted in an negligible amount of $Cr(III)_{(s)}$ formation during the oxidation reaction. In addition, the 250 mL glass vessels were covered by parafilm to avoid contact to air. Because OH^- is the only ligand to complex dissolved Cr(III), the precipitated Cr(III) solid is expected to exist as $Cr(OH)_{3(s)}$ with a maximum dissolved Cr(III) concentration of 0.1 μg/L at pH 7 based on the solubility product constant of $Cr(OH)_{3(s)}$ ($K_{sp} = 6.3 \times 10^{-31}$).[41] Furthermore, control experiments with pure $Cr(OH)_{3(s)}$ solid exhibited a much lower rate constant for Cr(VI) formation via HOCl oxidation (i.e., 0.2×10^{-3} vs 1.67×10^{-3} L·m^{-2}·min^{-1}; Figure 2) than $Cr(0)_{(s)}$. Therefore, the enhanced formation of $Cr(OH)_{3(s)}$ on the surface of $Cr(0)_{(s)}$ at higher pH inhibited Cr(VI) formation.

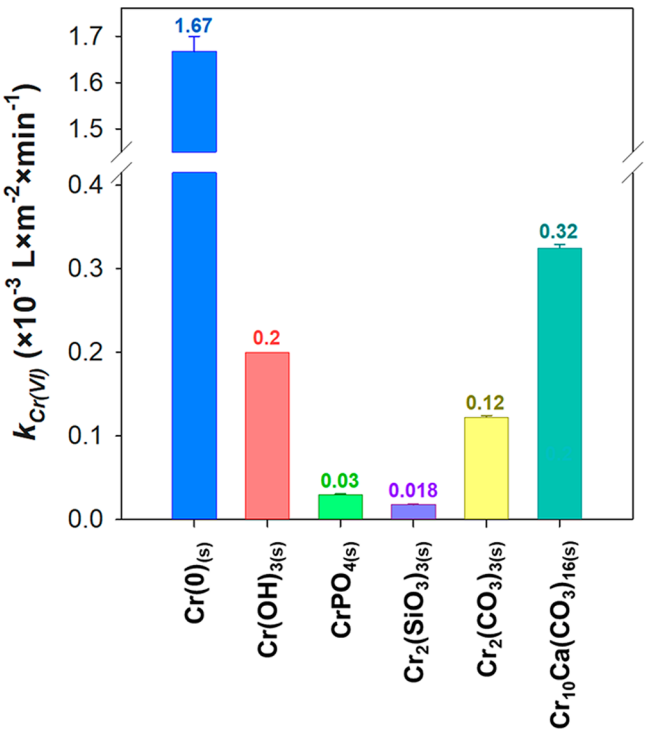

Figure 2. $k_{Cr(VI)}$ from the oxidation of different Cr solids by free chlorine at pH = 7 with 10 mM ionic strength. $[HOCl]_{TOT}$ = 20 mg Cl_2/L (0.282 mM); Cr solids = 440 mg/L.

Effect of Phosphate on Cr(VI) Formation. The impact of phosphate on Cr(VI) formation depended on the applied concentration (Figure 3A). When the phosphate dosage was increased from 0 to 0.1 mg/L as PO_4, the rate of Cr(VI) formation increased by 53% (1.7×10^{-3} vs 2.6×10^{-3} L·m^{-2}·min^{-1}; Figure 3B). The presence of phosphate was previously reported to block the active sites for malachite Cu_2CO_3 $(OH)_{2(s)}$ precipitation during the copper corrosion

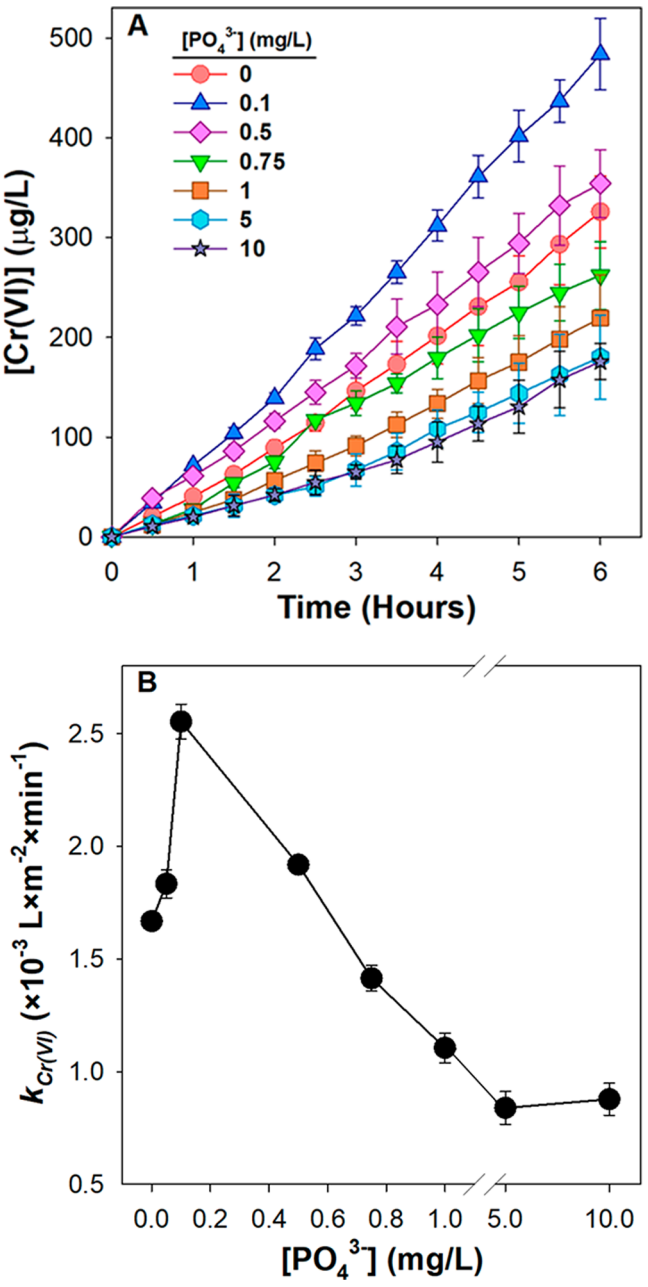

Figure 3. Six hour oxidation of $Cr(0)_{(s)}$ by free chlorine at different phosphate levels. $[HOCl]_{TOT}$ = 20 mg Cl_2/L (0.282 mM); $[Cr(0)_{(s)}]$ = 440 mg/L (8.46 mM); molar ratio of Cr(0)/HOCl = 30:1; pH = 7; ionic strength = 10 mM, [Ca] = 0 mg/L. (A) Cr(VI) formation; (B) $k_{Cr(VI)}$.

process, resulting in an increase in copper release.[42] Similarly, in the system with Cr solids, a low concentration of phosphate suppressed $Cr(OH)_{3(S)}$ formation on the surface of $Cr(0)_{(s)}$ because phosphate can compete with OH^- for adsorption sites on the surface $Cr(0)_{(s)}$, consequently decrease the surface concentration of OH^-, and suppress $Cr(OH)_{3(s)}$ formation. This surface reaction mechanism was supported by the observed $Cr(OH)_{3(s)}$ formation during the oxidation reaction. In the absence of phosphate, 0.38 mg/g $Cr(OH)_{3(s)}$ was formed on the surface of $Cr(0)_{(s)}$ after 6 h oxidation (Figure S4). When 0.1 mg/L phosphate was added to the system, $Cr(OH)_{3(s)}$ formation decreased by 53% (0.18 vs 0.38 mg/g). Therefore, 0.1 mg/L phosphate enhanced Cr(VI) formation by

https://doi.org/10.1021/acs.est.2c05324
Environ. Sci. Technol. 2023, 57, 18433−18442

decreasing $Cr(OH)_{3(s)}$ formation on the surface of $Cr(0)_{(s)}$. It was found that 0.5 mg/L phosphate had lower Cr(VI) formation than 0.1 mg/L phosphate, which was possibly due to $Cr(PO_4)_{(s)}$ beginning to form on the surface of $Cr(0)_{(s)}$. In addition, approximately 70% of phosphate was transferred from the aqueous phase to the solid phase at the end of the $Cr(0)_{(s)}$ oxidation reaction (Figure S5), which indicates the adsorption of phosphate during the reaction. There is little in the literature on how other aqueous species affected the OH^- adsorption. Previous studies showed that phosphate can decrease the adsorption of negatively charged species such as carbonate species, silicate, and citrate through competing for the adsorption sites.[43−45] Therefore, it is possible that the dominant anions in drinking water such as HCO_3^-, Cl^-, SO_4^{2-}, and NO_3^- may reduce OH^- adsorption due to the competitive adsorption.

In contrast, when the phosphate concentration was ≥0.75 mg/L, Cr(VI) formation was inhibited. $k_{Cr(VI)}$ was between 0.8 and 1.1 × 10^{-3} L·m^{-2}·min^{-1} with 0.75−10 mg/L phosphate (Figure 3B), 35−53% lower than that in the absence of phosphate. Accordingly, the concentration of Cr(III) solids on the surface of $Cr(0)_{(s)}$ was 28−38% higher than that without phosphate (Figure S6). Phosphate can react with dissolved Cr(III) to form insoluble $CrPO_{4(s)}$ with a K_{sp} of 7.2 × 10^{-18} (Table S1) (reaction 2)

$$Cr(III) + PO_4^{3-} \rightarrow CrPO_{4(s)} \quad K_{sp} = 7.2 \times 10^{-18} \qquad (R2)$$

The K_{sp} was calculated based on the 6 h of dissolution experiments to represent newly formed Cr(III) solids during the 6 h oxidation experiment. The K_{sp} of $CrPO_{4(s)}$ (7.2 × 10^{-18}) was much higher than that in the previous study (2.4 × 10^{-23}),[46] possibly due to the formation of a more soluble form of $CrPO_{4(s)}$ with a shorter duration of dissolution during the synthesis in this study.

Because $CrPO_{4(s)}$ solid exhibited a much lower reactivity than $Cr(0)_{(s)}$ to form Cr(VI) (0.03 × 10^{-3} vs 1.67 × 10^{-3} L·m^{-2}·min^{-1}) (Figure 2), formation of $CrPO_{4(s)}$ can inhibit Cr(VI) formation. The acid digestion result confirmed the formation of $CrPO_{4(s)}$ on the surface of $Cr(0)_{(s)}$. When 1 mg/L phosphate was added to the system, both $Cr(OH)_{3(s)}$ (0.31 mg/g as Cr(III)/Cr(0)) and $CrPO_{4(s)}$ (0.17 mg/g as Cr(III)/Cr(0)) were formed on the surface of $Cr(0)_{(s)}$ (Figure S4). In addition, although 10 mg/L phosphate could have more $CrPO_{4(s)}$ precipitation than 5 mg/L phosphate, some of the $CrPO_{4(s)}$ may detach from the $Cr(0)_{(s)}$, resulting in a comparable $Cr(0)_{(s)}$ surface area that is exposed to free chlorine. Thus, a similar inhibitory effect was observed at 5 and 10 mg/L phosphate.

Many studies have shown that the adsorption capacity of phosphate decreased with increasing pH. Three different studies showed that the adsorption of phosphate on different metal oxides decreased by approximate 25% when increasing two units of pH: goethite with pH from 6 to 8,[47] hydrous ferric oxide with pH from 6.5 to 8.5 (40 vs 32 mg/g),[48] and zirconium-modified coal gasification coarse slag with pH from 6 to 8 (16 vs 12 mg/g).[49] Assuming that the phosphate adsorption on $Cr(0)_{(s)}$ was affected to the same extent, it is estimated that 0.44 mg/L phosphate addition at pH 6 and 0.57 mg/L phosphate addition at pH 8 would enhance Cr(VI) formation. Thus, the critical phosphate level was approximately 0.5 mg/L across the typical pH range (6−8) in drinking water. However, the critical value should be further experimentally investigated due to the higher complexity of the drinking water distribution systems.

Effect of Silicate on Cr(VI) Formation. Statistical analysis showed that silicate (SiO_3^{2-}) had no significant effect on Cr(VI) formation at a concentration of ≤2.5 mg/L but exhibited an inhibitive effect on Cr(VI) formation at a concentration of ≥5 mg/L (Figure 4A). The rate constant with 10 mg/L silicate was 24% lower than without (1.3 × 10^{-3} vs. 1.7 × 10^{-3} L·m^{-2}·min^{-1}) (Figure 4B). Correspondingly, when the silicate concentration was ≥2.5 mg/L, the solid Cr(III) concentration on the surface of $Cr(0)_{(s)}$ was 66−97%

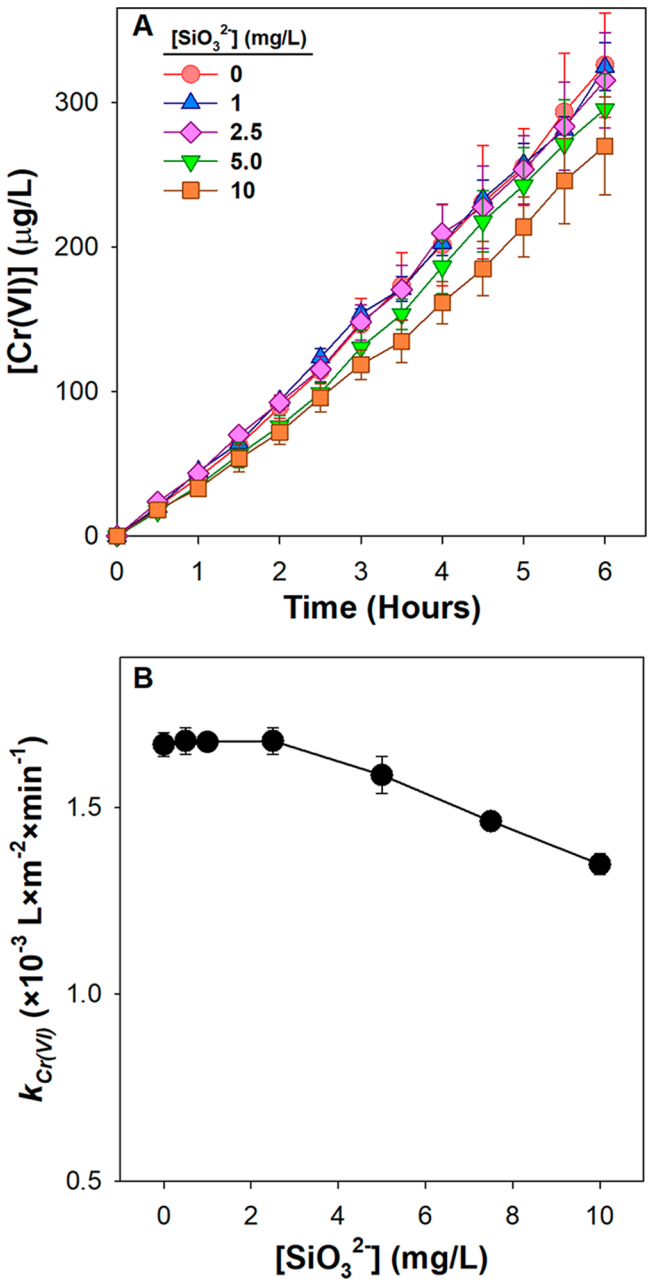

Figure 4. Six hour oxidation of $Cr(0)_{(s)}$ by free chlorine at different silicate levels. $[HOCl]_{TOT}$ = 20 mg Cl_2/L (0.282 mM); $[Cr(0)_{(s)}]$ = 440 mg/L (8.46 mM); molar ratio of Cr(0)/HOCl = 30:1; pH = 7; ionic strength = 10 mM, [Ca] = 0 mg/L. (A) Cr(VI) formation and (B) $k_{Cr(VI)}$. p value for Cr(VI) formation compared to that without silicate: 1 (0.9779), 2.5 (1.000), 5 (0.0100), and 10 mg/L (<0.0001).

https://doi.org/10.1021/acs.est.2c05324
Environ. Sci. Technol. 2023, 57, 18433−18442

higher than that without (0.63−0.75 vs 0.38 mg/g) (Figure S7). Silicate can react with dissolved Cr(III) to form insoluble $Cr_2(SiO_3)_{3(s)}$ with a K_{sp} of 9.8×10^{-36} (Table S1) (reaction 3)

$$2Cr(III) + 3SiO_3^{2-} \rightarrow Cr_2(SiO_3)_{3(s)} \quad K_{sp} = 9.8 \times 10^{-36} \tag{R3}$$

When 0.5 mg/L silicate was added to the system, only $Cr(OH)_{3(s)}$ (0.35 mg/g as Cr(III)/Cr(0)) was formed on the surface of the $Cr(0)_{(s)}$, which was comparable to the conditions without silicate (0.38 mg/g as Cr(III)/Cr(0)) (Figure S4). In the presence of 10 mg/L silicate, both $Cr_2(SiO_3)_{3(s)}$ (0.39 mg/g) and $Cr(OH)_{3(s)}$ (0.35 mg/g) were formed on the surface of $Cr(0)_{(s)}$ (Figure S4). Because $Cr_2(SiO_3)_{3(s)}$ had a much lower reactivity than the $Cr(0)_{(s)}$ reaction to form Cr(VI) (0.018×10^{-3} vs 1.67×10^{-3} L·m^{-2}·min^{-1}) (Figure 2), silicate can inhibit Cr(VI) formation through formation of $Cr_2(SiO_3)_{3(s)}$. The stoichiometry of the solid was confirmed. The Cr and Si concentrations in the digested sample were measured by ICP-MS, and the molar ratio of Cr to Si was close to 2:3.

Effects of Alkalinity and Calcium on Cr(VI) Formation. Increasing alkalinity to 50 mg $CaCO_3$/L can suppress Cr(VI) formation (Figure 5A and Figure S8). $k_{Cr(VI)}$ with 50 mg $CaCO_3$/L alkalinity was 24% lower than that without alkalinity (Figure 5B). Alkalinity promotes the formation of insoluble $Cr_2(CO_3)_{3(s)}$ with a K_{sp} of 1.1×10^{-45} (Table S1) (reaction R4)

$$2Cr(III) + 3CO_3^{2-} \rightarrow Cr_2(CO_3)_{3(s)} \quad K_{sp} = 1.1 \times 10^{-45} \tag{R4}$$

The equilibrium dissolved Cr(III) factor (α) was introduced to confirm the formation of $Cr_2(CO_3)_{3(s)}$. The value of α was calculated as the ratio of the dissolved Cr(III) concentration in equilibrium with a Cr(III) solid to the dissolved Cr(III) concentration in equilibrium with $Cr(OH)_{3(s)}$ at pH 7 as shown in eq 2

$$\alpha = \frac{Cr(III)_{dis1}}{Cr(III)_{dis0}} \tag{2}$$

where $Cr(III)_{dis1}$ is the dissolved Cr(III) concentration in equilibrium with different Cr(III) solids at pH 7 and $Cr(III)_{dis0}$ is the dissolved Cr(III) concentration in equilibrium with $Cr(OH)_{3(s)}$ at pH 7. The value of α indicated the sequence of the Cr(III) precipitation. When $\alpha > 1$, $Cr(OH)_{3(s)}$ will precipitate as the dominant species. When $\alpha < 1$, other Cr(III) solids will precipitate as dominant species.

The value of alpha predicts the dominant Cr(III) solids based on the equilibrated Cr(III) concentrations under different water chemistry from a thermodynamic point of view with the assumption that kinetics did not play an important role in the precipitation of different $Cr(III)_{(s)}$. The data showed that $Cr_2(CO_3)_{3(s)}$ has an α value significantly lower than 1 (Figure S9); therefore, $Cr_2(CO_3)_{3(s)}$ was the dominant Cr(III) solid on the surface of Cr(0) when an alkalinity of 10−200 mg $CaCO_3$/L was added into the system. Because $Cr_2(CO_3)_{3(s)}$ has a much lower reactivity than Cr(0) to form Cr(VI) (0.12×10^{-3} vs 1.67×10^{-3} L·m^{-2}·min^{-1}; Figure 2), formation of $Cr_2(CO_3)_{3(s)}$ inhibited Cr(VI) formation.

Under the same alkalinity condition, adding 200 mg/L calcium decreased Cr(VI) formation further by 7−19%, exhibited by lower $k_{Cr(VI)}$ values (Figure 5B). Thus, calcium

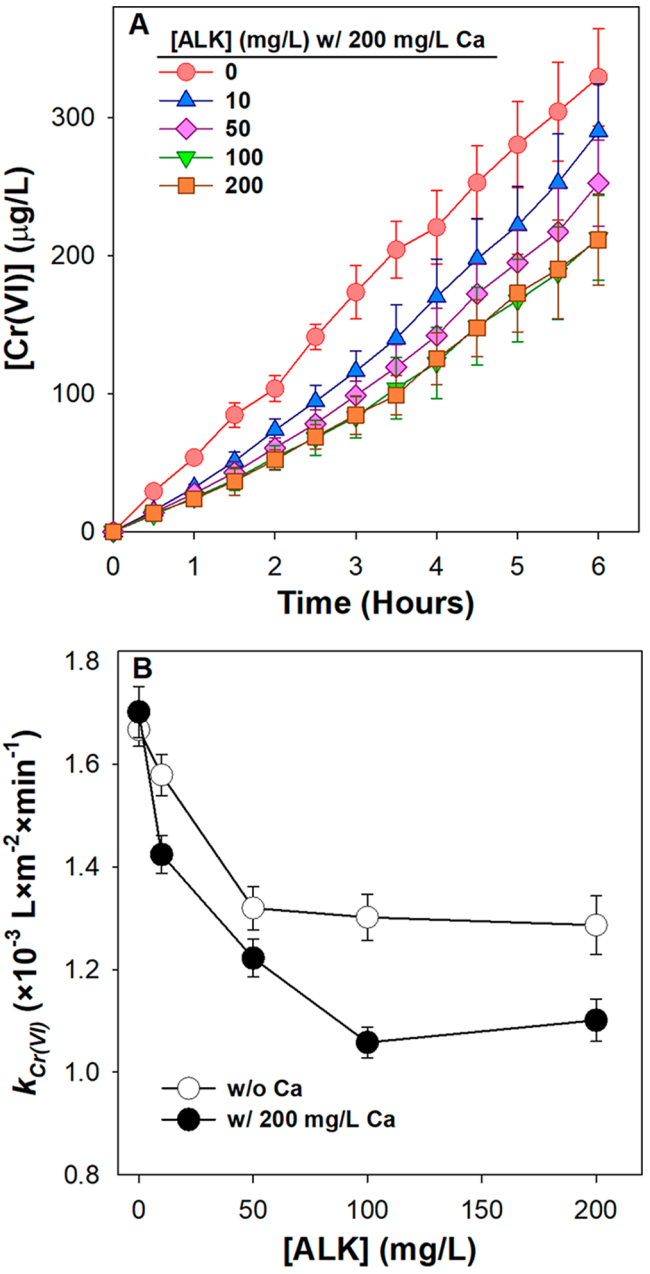

Figure 5. Six hour oxidation of $Cr(0)_{(s)}$ by free chlorine at different alkalinity levels (0−200 mg/L as $CaCO_3$) with and without 200 mg/L Ca. $[HOCl]_{TOT}$ = 20 mg Cl_2/L (0.282 mM); $[Cr(0)_{(s)}]$ = 440 mg/L (8.46 mM); molar ratio of Cr(0)/HOCl = 30:1; pH = 7; ionic strength = 10 mM: (A) Cr(VI) formation and (B) $k_{Cr(VI)}$.

and alkalinity together had a synergistic inhibitive effect on Cr(VI) formation by forming $Cr_{10}Ca(CO_3)_{16(s)}$ with a K_{sp} of 1×10^{-2} [50] (Table S1) (Reaction R5)

$$10Cr(III) + Ca^{2+} + 16CO_3^{2-} \rightarrow Cr_{10}Ca(CO_3)_{16(s)} \quad K_{sp} = 1 \times 10^{-250} \tag{R5}$$

The value of α for $Cr_{10}Ca(CO_3)_{16(s)}$ in the presence of 200 mg/L calcium was significantly lower than that without (3.5×10^{-5}−2.9×10^{-7} vs 1.2×10^{-3}−1.4×10^{-5}) (Figure S9); thus, $Cr_{10}Ca(CO_3)_{16(s)}$ would precipitate prior to $Cr_2(CO_3)_{3(s)}$. The acid digestion confirmed that $Cr_{10}Ca(CO_3)_{16(s)}$ was formed on the surface of $Cr(0)_{(s)}$ with 200 mg/L Ca and 200 mg/L

https://doi.org/10.1021/acs.est.2c05324
Environ. Sci. Technol. 2023, 57, 18433−18442

alkalinity (Figure S4). Because $Cr_{10}Ca(CO_3)_{16(s)}$ has a much lower reactivity than the $Cr(0)_{(s)}$ reaction to form Cr(VI) (3.2×10^{-5} vs 1.67×10^{-3} $L{\cdot}m^{-2}{\cdot}min^{-1}$) (Figure 2), formation of $Cr_{10}Ca(CO_3)_{16(s)}$ further inhibited Cr(VI) formation. In addition, without alkalinity, calcium alone (0−300 mg/L Ca^{2+}) had no effect on Cr(VI) formation through oxidation of $Cr(0)_{(s)}$ by chlorine (Figure S10) because calcium alone does not induce the formation of additional surface solid (Figure S4). The dissolution time was chosen as 6 h because the dissolved Cr(III) concentrations reached plateaus at 6 h as shown in Figure S2.

In all of the experiments, the Cr(VI) formation rates were constant throughout the reactions (Figures 1A, 3A, 4A, and 5A). When $Cr(0)_{(s)}$ reacts with free chlorine, $Cr(III)_{(s)}$ can form on the surface of $Cr(0)_{(s)}$, and the $Cr(III)_{(s)}$ can further react with free chlorine to form Cr(VI). The production and consumption of Cr(III) solids was a dynamic process reaching steady state in a short time, resulting in a constant Cr(III) steady-state concentration on the surface of $Cr(0)_{(s)}$. Thus, the inhibitive effect of $Cr(III)_{(s)}$ was constant during a majority of the reaction time, leading to a constant Cr(VI) formation rate.

Consumption of Free Chlorine. Free chlorine had a pK of 7.6; thus, HOCl was the dominant species when pH was lower than 7.6 and OCl^- was the dominant species when pH was higher than 7.6. HOCl can change to Cl_2O with an equilibrium constant (K) of 8.74×10^{-3} M^{-1} at 25 °C.[50] In equilibrium at pH 6, although the Cl_2O concentration was approximately 6 orders of magnitude lower than the HOCl concentration (6.5×10^{-10} vs 2.73×10^{-4} M), Cl_2O may still play a significant role for the oxidative formation of Cr(VI) due to its high reaction activity.[51] In this study, Cr(VI) formation was due to oxidation of all of the chlorine species, and their relative contributions were not further investigated.

For all reactions, less than 20% of the free chlorine were consumed after the 6 h of reaction. For example, 1.7−2.5 mg/L (8.5−12.5%) free chlorine was consumed after the 6 h reaction at different pHs (Figure S11). For the consumed free chlorine, 54−63% was due to oxidation of $Cr(0)_{(s)}$ to form Cr(VI), and the rest was mainly due to oxidation of $Cr(0)_{(s)}$ to form $Cr(III)_{(s)}$ on the surface of $Cr(0)_{(s)}$ and the possible autocatalytic decay of chlorine. The oxidation of $Cr(III)_{(s)}$ by chlorine can generate Cr(V) intermediate species in the form of Cr(V) oxide, and the Cr(V) oxide can generate dissolved oxygen by quickly decomposing to $Cr(III)_{(s)}$.[36]

Mechanisms of the Inhibition on Cr(VI) Formation. An increase in pH was previously reported to modestly enhance Cr(VI) formation during oxidation of $Cr(III)_{(s)}$ solids by free chlorine due to changes of reactive $Cr(III)_{(s)}$ surface hydroxo species.[36] In contrast, Cr(VI) formation was observed to decrease with increasing pH during $Cr(0)_{(s)}$ oxidation by free chlorine. The opposite pH trend strongly suggests that oxidation of $Cr(III)_{(s)}$ was not the rate-limiting reaction for Cr(VI) formation in the system with $Cr(0)_{(s)}$ and free chlorine. In addition, both $Cr(0)_{(s)}$ and $Cr(III)_{(s)}$ coexisted in the naturally formed iron corrosion scales, and $Cr(0)_{(s)}$ was found to mainly contribute to the fast Cr(VI) formation when the iron corrosion scales reacted with free chlorine.[15] As a result, the one-step reaction of direct $Cr(0)_{(s)}$ oxidation to Cr(VI) by free chlorine is likely the dominant pathway for Cr(VI) formation.

In this study, $Cr(0)_{(s)}$ exhibited a Cr(VI) formation rate constant that was 1−2 orders of magnitude higher than that for Cr(III) solids (Figure 2); thus, it is possible that a fast one-step $Cr(0)_{(s)}$ oxidation to Cr(VI) was the dominant reaction to form Cr(VI) (Mechanism 1). In addition, the surface speciation measurements of Cr(III) solid (Figures S3, S6, and S7) confirmed that different less reactive Cr(III) solids were formed during oxidation of $Cr(0)_{(s)}$ by free chlorine when pH, silicate, phosphate, calcium, and alkalinity were adjusted to desirable levels. This observation supported the second Cr(VI) formation mechanism (Mechanism 2) that Cr(VI) formation via $Cr(0)_{(s)}$ oxidation involved two steps: $Cr(0)_{(s)}$ oxidation to $Cr(III)_{(s)}$ and then $Cr(III)_{(s)}$ oxidation to Cr(VI) (k_{III}).

To quantitatively evaluate the relative importance of Mechanisms 1 and 2 on Cr(VI) formation, the branching ratio of Mechanism 1 was calculated (eq 3)

$$\text{Branching ratio of Mechanism 1} = \frac{[S_{Cr(0)}][k_0]}{[S_{Cr(0)}][k_0] + \Sigma[S_{Cr(III)}][k_{III}]} \quad (3)$$

where $S_{Cr(0)}$ and $S_{Cr(III)}$ are the percentages of $Cr(0)_{(s)}$ surface area covered by $Cr(0)_{(s)}$ and $Cr(III)_{(s)}$ and k_0 and k_{III} are the surface-area-normalized second-order rate constants for Cr(VI) formation from Cr(0) and Cr(III) solids. The details of the calculation of $S_{Cr(0)}$ and $S_{Cr(III)}$ and the branching ratio are shown in Text S4, and the results are shown in Figures S12 and S13, respectively. The branching ratio of Mechanism 1 (one-step reaction) was overwhelmingly higher (i.e., 0.95−0.98 in most conditions; Figure S13). Overall, these results confirmed that the dominant mechanism for Cr(VI) formation was the one-step oxidation of $Cr(0)_{(s)}$ to Cr(VI). In addition, previous studies showed that Cr(V), as a Cr intermediate species, could be formed during the redox reaction.[52,53] However, the Cr intermediate species was not investigated in this study. The proposed one-step oxidation mechanism does not rule out the possibility that a Cr intermediate species could be formed and was quickly oxidized to Cr(VI), which may contribute a significant amount of Cr(VI).

Although the Cr(III) solids had different reactivities with HOCl, $k_{Cr(VI)}$ apparently has an inverse relationship to the Cr(III) solid concentration on the surface of $Cr(0)_{(s)}$ (Figure 6). On the basis of their low branching ratios, Cr(III) solids were not the dominant source of Cr(VI) formation (Figure S13), but they can significantly inhibit Cr(VI) formation through reducing the contact area between $Cr(0)_{(s)}$ and chlorine, decreasing Cr(VI) formation. For example, $S_{Cr(0)}$ decreased from 75% to 35% when 200 mg/L Ca^{2+} was added, and the alkalinity was increased from 0 to 200 mg $CaCO_3$/L (Figure S12). Overall, Cr(III) solids on the surface of $Cr(0)_{(s)}$ are critical for Cr(VI) formation through oxidation of $Cr(0)_{(s)}$ by chlorine; thus, the control strategy for Cr(VI) formation should focus on the Cr(III) solids formation on the surface of $Cr(0)_{(s)}$.

Environmental Implications. Cr(VI) is a carcinogen, and its presence in drinking water even at a trace level poses a great public health risk. It is possible that more rigorous regulations for Cr(VI) will be enforced in the future. In addition, to solve the issue of water scarcity, more desalinated water would be used as drinking water sources, and the desalinated water with higher bromide as a catalyst would enhance Cr(VI) formation by several times.[15,36] Thus, Cr(VI) control is important for the drinking water distribution systems.

On the basis of realistic chemical conditions in the drinking water distribution system and using kinetics data obtained

https://doi.org/10.1021/acs.est.2c05324
Environ. Sci. Technol. 2023, 57, 18433−18442

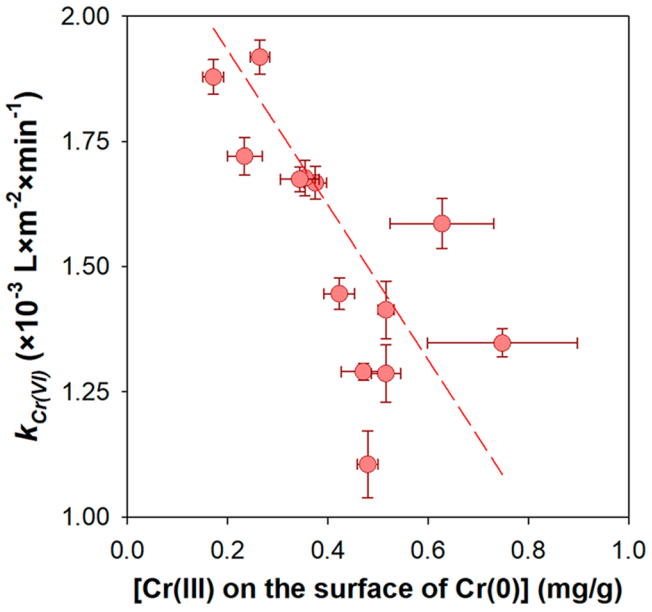

Figure 6. Relationship between the $k_{Cr(VI)}$ and the Cr(III) solids using all available data of Cr(III) solid formation on the surface of $Cr(0)_{(s)}$.

from this study, a simple adjustment of pH from 6 to 8 is predicted to decrease the formation of Cr(VI) by 31% (Figure 7). Combined with increasing the pH from 6 to 7, dosing 1

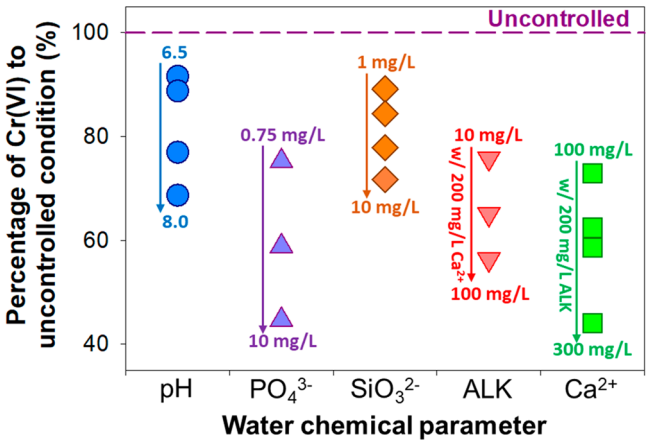

Figure 7. Relative Cr(VI) concentration under different control strategies to uncontrolled conditions in drinking water distribution systems with 0.68 mg/L bromide in U.S. source waters. Control was at pH = 6, and other conditions were at pH = 7 unless specified.

mg/L phosphate or 10 mg/L silicate can reduce Cr(VI) formation by 41% or 28%, respectively (Figure 7). Phosphate is reportedly dosed at 0.2−6 mg/L as PO_4 in drinking water to control corrosion and lead release in England and the United States.[54,55] In contrast, 5−25 mg/L as SiO_2 of silicate is used primarily for iron/manganese sequestration in drinking water.[33] Therefore, phosphate or silicate addition can be applied to inhibit Cr(VI) formation. Furthermore, since increasing the water alkalinity from 10 to 100 mg/L in the presence of 200 mg/L of background calcium reduced Cr(VI) formation by 26% (Figure 7), Cr(VI) formation could potentially be lowered further if a higher pH combined with phosphate dosing in combination with calcium and alkalinity were implemented.

Increasing pH/alkalinity in drinking water treatment plants can be a viable control strategy to reduce Cr(VI) formation. Unlike silicate, phosphate has both an enhanced and an inhibitive effect on Cr(VI) formation; thus, more attention should be paid to the use of phosphate in real DWDSs. In the future, it may be necessary to reduce Cr(VI) in drinking water further to protect public health. This study provides knowledge and understanding of Cr(VI) formation kinetics and related mechanisms in drinking waters with different chemistry.

In addition, Fe(II) and organic matter may exist in the iron corrosion scales to compete with Cr solids for the consumption of free chlorine; thus, they could reduce Cr(VI) formation.[15] Fe(III) in the iron corrosion scales could precipitate out Cr(III) to form Cr(III)−Fe(III) hydroxides. MnO_2 as a catalyst in the corrosion scales could accelerate the oxidation of Cr solids to form Cr(VI).[56] Thus, when applying these control strategies in a real drinking water distribution system, more research effort should be taken to understand the complexity of the redox chemistry in the drinking water distribution systems in the future.

■ ASSOCIATED CONTENT

Supporting Information

The Supporting Information is available free of charge at https://pubs.acs.org/doi/10.1021/acs.est.2c05324.

Synthesis of different Cr(III) solids; Cr(III) solids concentration on the Cr(0) after 6 h oxidation reaction at different pH, phosphate, calcium, and alkalinity; calculation of maximum dissolved Cr(VI) factor and K_{sp} of different Cr(III) solids; kinetic model for the prediction of Cr(VI) concentrations in drinking water distribution systems (PDF)

■ AUTHOR INFORMATION

Corresponding Author

Haizhou Liu − *Department of Chemical and Environmental Engineering, University of California at Riverside, Riverside, California 92521, United States;* orcid.org/0000-0003-4194-2566; Phone: (951) 827-2076; Email: haizhou@engr.ucr.edu; Fax: (951) 827-5696

Author

Cheng Tan − *Department of Chemical and Environmental Engineering, University of California at Riverside, Riverside, California 92521, United States;* orcid.org/0000-0001-5878-6542

Complete contact information is available at: https://pubs.acs.org/10.1021/acs.est.2c05324

Notes

The authors declare no competing financial interest.

■ ACKNOWLEDGMENTS

This research was supported by the U.S. National Science Foundation CAREER Program (CBET-1653931). We thank Soham Shah for BET analysis, group member Liang Wu for assistance in this project at UC Riverside, and Ken Ishida at Orange County Water District for his assistance in the preparation of the manuscript.

REFERENCES

(1) Krishnamurthy, S.; Wilkens, M. M. Environmental Chemistry of Chromium. *Northeast. Geol.* **1994**, *16* (1), 14−17.
(2) Saha, R.; Nandi, R.; Saha, B. Sources and Toxicity of Hexavalent Chromium. *J. Coord. Chem.* **2011**, *64* (10), 1782−1806.
(3) Salnikow, K.; Zhitkovich, A. Genetic and Epigenetic Mechanisms in Metal Carcinogenesis and Cocarcinogenesis: Nickel, Arsenic, and Chromium. *Chem. Res. Toxicol.* **2008**, *21* (1), 28−44.
(4) Liu, H.; Yu, X. Hexavalent Chromium in Drinking Water: Chemistry, Challenges and Future Outlook on Sn(II)- and Photocatalyst-Based Treatment. *Front. Environ. Sci. Eng.* **2020**, *14* (5), 88.
(5) EPA.National Primary Drinking Water Regulations; Final Rule. *Fed. Regist.***1991**, *56*, 3536−3537.
(6) Brown, E. G.; Alexeeff, G. V. Hexavalent Chromium (Cr VI). *Public Health Goals for Chemicals in Drinking Water* **2011**, 1−162.
(7) *Unregulated Contaminant Monitoring Rule 3 (UCMR 3)*; United States Environmental Protection Agency, 2015.
(8) Zhitkovich, A. Chromium in Drinking Water: Sources, Metabolism, and Cancer Risks. *Chem. Res. Toxicol.* **2011**, *24* (10), 1617−1629.
(9) Oze, C.; Bird, D. K.; Fendorf, S. Genesis of Hexavalent Chromium from Natural Sources in Soil and Groundwater. *Proc. Natl. Acad. Sci. U. S. A.* **2007**, *104* (16), 6544−6549.
(10) Loock, M. M.; Beukes, J. P.; van Zyl, P. G. Conductivity as an Indicator of Surface Water Quality in the Proximity of Ferrochrome Smelters in South Africa. *Water SA* **2015**, *41* (5), 705−711.
(11) McNeill, L. S.; McLean, J. E.; Parks, J. L.; Edwards, M. A. Hexavalent Chromium Review, Part 2: Chemistry, Occurrence, and Treatment. *J. Am. Water Works Assoc.* **2012**, *104* (7), E395−E405.
(12) Moffat, I.; Martinova, N.; Seidel, C.; Thompson, C. M. Hexavalent Chromium in Drinking Water. *J. Am. Water Works Assoc.* **2018**, *110* (5), E22−E35.
(13) Owlad, M.; Aroua, M. K.; Daud, W. A. W.; Baroutian, S. Removal of Hexavalent Chromium-Contaminated Water and Wastewater: A Review. *Water. Air. Soil Pollut.* **2009**, *200* (1−4), 59−77.
(14) Świetlik, J.; Raczyk-Stanisławiak, U.; Piszora, P.; Nawrocki, J. Corrosion in Drinking Water Pipes: The Importance of Green Rusts. *Water Res.* **2012**, *46* (1), 1−10.
(15) Tan, C.; Avasarala, S.; Liu, H. Hexavalent Chromium Release in Drinking Water Distribution Systems: New Insights into Zerovalent Chromium in Iron Corrosion Scales. *Environ. Sci. Technol.* **2020**, *54* (20), 13036−13045.
(16) Chebeir, M.; Chen, G.; Liu, H. Emerging Investigators Series: Frontier Review: Occurrence and Speciation of Chromium in Drinking Water Distribution Systems. *Environ. Sci. Water Res. Technol.* **2016**, *2* (6), 906−914.
(17) Lytle, D. A.; Schock, M. R.; Clement, J. A.; Spencer, C. M. Using Aeration for Corrosion Control: Under the Right Initial Water Quality Conditions, Aeration Proves a Suitable Alternative for Reducing Lead and Copper Corrosion. *J./Am. Water Work. Assoc.* **1998**, *90* (3), 74−88.
(18) Pinto, J. A.; McAnally, A. S.; Flora, J. R.V. Evaluation of Lead and Copper Corrosion Control Techniques. *J. Environ. Sci. Health, Part A: Toxic/Hazard. Subst. Environ. Eng.*. **1997**, *32* (1), 31−53.
(19) Lasheen, M. R.; Sharaby, C. M.; El-Kholy, N. G.; Elsherif, I. Y.; El-Wakeel, S. T. Factors Influencing Lead and Iron Release from Some Egyptian Drinking Water Pipes. *J. Hazard. Mater.* **2008**, *160* (2−3), 675−680.
(20) Tam, Y. S.; Elefsiniotis, P. Corrosion Control in Water Supply Systems: Effect of pH, Alkalinity, and Orthophosphate on Lead and Copper Leaching from Brass Plumbing. *J. Environ. Sci. Health, Part A: Toxic/Hazard. Subst. Environ. Eng.* **2009**, *44* (12), 1251−1260.
(21) Karalekas, P. C.; Ryan, C. R.; Taylor, F. B. Control of Lead, Copper, and Iron Pipe Corrosion in Boston. *J./Am. Water Work. Assoc.* **1983**, *75* (2), 92−95.
(22) Pedeferri, P. General Principles of Corrosion. *Corrosion Science and Engineering; Engineering Materials; Springer International Publishing: Cham* **2018**, 1−16.
(23) Cherney, D. P.; Duirk, S. E.; Tarr, J. C.; Collette, T. W. Monitoring the Speciation of Aqueous Free Chlorine from pH 1 to 12 with Raman Spectroscopy to Determine the Identity of the Potent Low-pH Oxidant. *Appl. Spectrosc.* **2006**, *60* (7), 764−772.
(24) Lee, G.; Hering, J. G. Oxidative Dissolution of Chromium(III) Hydroxide at pH 9, 3, and 2 with Product Inhibition at PH 2. *Environ. Sci. Technol.* **2005**, *39* (13), 4921−4928.
(25) Hu, J.; Dong, H.; Xu, Q.; Ling, W.; Qu, J.; Qiang, Z. Impacts of Water Quality on the Corrosion of Cast Iron Pipes for Water Distribution and Proposed Source Water Switch Strategy. *Water Res.* **2018**, *129*, 428−435.
(26) Li, M.; Wang, Y.; Liu, Z.; Sha, Y.; Korshin, G. V.; Chen, Y. Metal-Release Potential from Iron Corrosion Scales under Stagnant and Active Flow, and Varying Water Quality Conditions. *Water Res.* **2020**, *175*, 115675.
(27) Tang, C.; Godskesen, B.; Aktor, H.; van Rijn, M.; Kristensen, J. B.; Rosshaug, P. S.; Albrechtsen, H. J.; Rygaard, M. Procedure for Calculating the Calcium Carbonate Precipitation Potential (CCPP) in Drinking Water Supply: Importance of Temperature, Ionic Species and Open/Closed System. *Water (Switzerland)* **2021**, *13* (1), 42.
(28) EPA.*Optimal Corrosion Control Treatment Evaluation Technical Recommendations for Primacy Agencies and Public Water Systems*; U.S. Environmental Protection Agency, 2016; Vol. *6*, p 140.
(29) Li, B.; Trueman, B. F.; Munoz, S.; Locsin, J. M.; Gagnon, G. A. Impact of Sodium Silicate on Lead Release and Colloid Size Distributions in Drinking Water. *Water Res.* **2021**, *190*, 116709.
(30) Yohai, L.; Vázquez, M.; Valcarce, M. B. Phosphate Ions as Corrosion Inhibitors for Reinforcement Steel in Chloride-Rich Environments. *Electrochim. Acta* **2013**, *102*, 88−96.
(31) Bae, Y.; Pasteris, J. D.; Giammar, D. E. The Ability of Phosphate to Prevent Lead Release from Pipe Scale When Switching from Free Chlorine to Monochloramine. *Environ. Sci. Technol.* **2020**, *54* (2), 879−888.
(32) Thompson, J. L.; Scheetz, B. E.; Schock, M. R.; Lytle, D. A.*Sodium Silicate as Corrosion Inhibitor, Report 12*; PQ Corp.: Valley Forge, PA, 1997.
(33) Robinson, R. B.; Reed, G. D.; Frazier, B. Iron and Manganese Sequestration Facilities Using Sodium Silicate. *J./Am. Water Work. Assoc.* **1992**, *84* (2), 77−82.
(34) Mcneill, L. S.; Edwards, M. Iron Pipe Corrosion in Distribution Systems. *J./Am. Water Work. Assoc.* **2001**, *93* (7), 88−100.
(35) Rushing, J. C.; McNeill, L. S.; Edwards, M. Some Effects of Aqueous Silica on the Corrosion of Iron. *Water Res.* **2003**, *37* (5), 1080−1090.
(36) Chebeir, M.; Liu, H. Kinetics and Mechanisms of Cr(VI) Formation via the Oxidation of Cr(III) Solid Phases by Chlorine in Drinking Water. *Environ. Sci. Technol.* **2016**, *50* (2), 701−710.
(37) Chebeir, M.; Liu, H. Oxidation of Cr(III)-Fe(III) Mixed-Phase Hydroxides by Chlorine: Implications on the Control of Hexavalent Chromium in Drinking Water. *Environ. Sci. Technol.* **2018**, *52* (14), 7663−7670.
(38) USEPA*Method 3050B Acid Digestion of Sediments, Sludges and Soils, Revision 2*; Environmental Protection Agency: Washington, DC, 1996.
(39) Bruno, L.*Standard Methods for the Examination of Water and Wastewater*, 23rd ed.; Water Environment Federation, 2017; Vol. *53*.
(40) Russell, B.; Goddard, S. L.; Mohamud, H.; Pearson, O.; Zhang, Y.; Thompkins, H.; Brown, R. J. C. Applications of Hydrogen as a Collision and Reaction Cell Gas for Enhanced Measurement Capability Applied to Low Level Stable and Radioactive Isotope Detection Using ICP-MS/MS. *J. Anal. At. Spectrom.* **2021**, *36* (12), 2704−2714.
(41) Chen, G.; Yang, L.; Chen, J.; Miki, T.; Li, S.; Bai, H.; Nagasaka, T. Competitive Mechanism and Influencing Factors for the Simultaneous Removal of Cr(III) and Zn(II) in Acidic Aqueous Solutions Using Steel Slag: Batch and Column Experiments. *J. Clean. Prod.* **2019**, *230*, 69−79.

https://doi.org/10.1021/acs.est.2c05324
Environ. Sci. Technol. 2023, 57, 18433−18442

(42) Dartmann, J.; Sadlowsky, B.; Dorsch, T.; Johannsen, K. Copper Corrosion in Drinking Water Systems - Effect of pH and Phosphate-Dosage. *Mater. Corros.* **2010**, *61* (3), 189−198.
(43) Mendez, J. C.; Hiemstra, T. Carbonate Adsorption to Ferrihydrite: Competitive Interaction with Phosphate for Use in Soil Systems. *ACS Earth Sp. Chem.* **2019**, *3* (1), 129−141.
(44) Chen, P.; Song, D.; Zhang, X.; Xie, Q.; Zhou, Y.; Liu, H.; Xu, L.; Chen, T.; Rosso, K. M. Understanding Competitive Phosphate and Silicate Adsorption on Goethite by Connecting Batch Experiments with Density Functional Theory Calculations. *Environ. Sci. Technol.* **2022**, *56* (2), 823−834.
(45) Geelhoed, J. S.; Hiemstra, T.; Van Riemsdijk, W. H. Competitive Interaction between Phosphate and Citrate on Goethite. *Environ. Sci. Technol.* **1998**, *32* (14), 2119−2123.
(46) Zhang, Z.; Li, B.; Wicaksana, F.; Yu, W.; Young, B.Comparison of Struvite and K-Struvite for Pb and Cr Immobilisation in Contaminated Soil. *SSRN J.***2022**. DOI: 10.2139/ssrn.4112031.
(47) Sabur, M. A.; Parsons, C. T.; Maavara, T.; Van Cappellen, P. Effects of pH and Dissolved Silicate on Phosphate Mineral-Water Partitioning with Goethite. *ACS Earth Sp. Chem.* **2022**, *6* (1), 34−43.
(48) Zhang, H.; Elskens, M.; Chen, G.; Chou, L. Phosphate Adsorption on Hydrous Ferric Oxide (HFO) at Different Salinities and pHs. *Chemosphere* **2019**, *225*, 352−359.
(49) Yang, B.; Han, F.; Xie, Z.; Yang, Z.; Jiang, F.; Yang, S.; Li, Y. Study on Adsorption of Phosphate from Aqueous Solution by Zirconium Modified Coal Gasification Coarse Slag. *RSC Adv.* **2022**, *12* (27), 17147−17157.
(50) Sivey, J. D.; McCullough, C. E.; Roberts, A. L. Chlorine Monoxide (Cl_2O) and Molecular Chlorine (Cl_2) as Active Chlorinating Agents in Reaction of Dimethenamid with Aqueous Free Chlorine. *Environ. Sci. Technol.* **2010**, *44* (9), 3357−3362.
(51) Sivey, J. D.; Roberts, A. L. Assessing the Reactivity of Free Chlorine Constituents Cl_2, Cl_2O, and HOCl toward Aromatic Ethers. *Environ. Sci. Technol.* **2012**, *46* (4), 2141−2147.
(52) Chebeir, M.; Liu, H. Kinetics and Mechanisms of Cr(VI) Formation via the Oxidation of Cr(III) Solid Phases by Chlorine in Drinking Water. *Environ. Sci. Technol.* **2016**, *50* (2), 701−710.
(53) Dong, H.; Wei, G.; Cao, T.; Shao, B.; Guan, X.; Strathmann, T. J. Insights into the Oxidation of Organic Cocontaminants during Cr(VI) Reduction by Sulfite: The Overlooked Significance of Cr(V). *Environ. Sci. Technol.* **2020**, *54* (2), 1157−1166.
(54) Cardew, P. T. Measuring the Benefit of Orthophosphate Treatment on Lead in Drinking Water. *J. Water Health* **2009**, *7* (1), 123−131.
(55) McNeil, L. S.; Edwards, M. Phosphate Inhibitor Use at US Utilities. *J. Am. Water Works Assoc.* **2002**, *94* (7), 57−63.
(56) Pan, W.; Pan, C.; Bae, Y.; Giammar, D. Role of Manganese in Accelerating the Oxidation of Pb(II) Carbonate Solids to Pb(IV) Oxide at Drinking Water Conditions. *Environ. Sci. Technol.* **2019**, *53* (12), 6699−6707.

https://doi.org/10.1021/acs.est.2c05324
Environ. Sci. Technol. 2023, 57, 18433−18442